Available online at www.sciencedirect.com
SCIENCE DIRECT
Polymer 46 (2005) 3462–3471
polymer
www.elsevier.com/locate/polymer

Influence of compatibilizer and processing conditions on the dispersion of nanoclay in a polypropylene matrix

W. Lertwimolnun, B. Vergnes*

CEMEF, Ecole des Mines de Paris, UMR CNRS 7635, BP 207, 06904 Sophia Antipolis, Cedex, France

Accepted 7 January 2005
Available online 23 March 2005

Abstract

Polypropylene/organoclay nanocomposites have been prepared via direct melt intercalation in an internal mixer. Maleic anhydride grafted polypropylene (PP-g-MA) was used as a compatibilizer to improve the dispersability of the clay. The structures of nanocomposites have been characterized by X-ray diffraction, transmission electron microscopy and rheometry in small amplitude oscillatory shear. The effects of concentration of PP-g-MA and processing parameters were investigated. Wide angle X-ray diffraction shows that the interlayer spacing increases with the concentration of PP-g-MA, but is not significantly influenced by processing conditions. The study of linear viscoelastic properties shows that the storage modulus G' is very sensitive to the microstructure of the nanocomposite. A Carreau–Yasuda law with a yield stress is proposed to describe the rheological behavior of these materials. Applications to the twin screw extrusion process are also presented.

Keywords: Nanoclay; Processing conditions; Dispersion

1. Introduction

Organically modified layered silicates (organoclay) are increasingly used for reinforcement of polymeric materials. It has been reported that the dispersion of such minerals at the level of a few nanometers induces a significant improvement in mechanical properties, flame resistance and barrier properties, compared with the pure polymer [1,2]. In addition, these improvements may be obtained with low clay loading (typically less than 5%). There are several techniques used for dispersing organoclay at a nanoscopic scale, including the addition of organoclay during polymerization (in situ method), or to a solvent swollen polymer (solution blending), or to a polymer melt (melt intercalation method), as described in recent reviews [1–3].

According to these techniques, two ideal structures defined as intercalated nanocomposite and exfoliated nanocomposite are commonly used to describe the state of dispersion [1,2]. In the former, the polymer chains are intercalated between the silicate layers, resulting in a well ordered alternating layered silicates and polymer chains. In contrast, in the exfoliated structure, the individual clay layers are dispersed in the polymer matrix. The term conventional composite or microcomposite is also used to describe the structure of nanocomposite containing the clay tactoids with the layers aggregated in unintercalated form.

One of the most commonly used organically layered silicates is derived from montmorillonite (MMT). Its structure is made of several stacked layers, with a layer thickness around 0.96 nm and a lateral dimension of 100–200 nm [4,5]. These layers organize themselves to form the stacks with a regular gap between them, called interlayer or gallery. The sum of the single layer thickness (0.96 nm) and the interlayer represents the repeat unit of the multilayer material, called *d*-spacing or basal spacing (d_{001}), and is calculated from the (001) harmonics obtained from X-ray diffraction patterns.

The clay is naturally a hydrophilic material, which makes it difficult to exfoliate in a polymer matrix. Therefore, the surface treatment of silicate layers is necessary to render its surface more hydrophobic, which facilitates exfoliation. Generally, this can be done by ion-exchange reactions with cationic surfactants, including primary, secondary, tertiary

* Corresponding author. Tel.: +33 4 93 95 74 63; fax: +33 4 93 65 43 04.
E-mail address: bruno.vergnes@ensmp.fr (B. Vergnes).

0032-3861/$ - see front matter © 2005 Elsevier Ltd. All rights reserved.
doi:10.1016/j.polymer.2005.02.018

and quaternary alkylammonium cations [6,7]. This modification also leads to expand the basal spacing between the silicate layers due to the presence of alkyl chain intercalated in the interlayer. For polymer containing polar functional groups, an alkylammonium surfactant is adequate to promote the nanocomposite formation. However, in the case of polypropylene, it is frequently necessary to use a compatibilizer, such as maleic anhydride modified polypropylene (PP-g-MA). Kawasumi et al. [8], Kato et al. [9] and Hasegawa et al. [10] showed that there are two important factors to achieve the exfoliation of the clay layer silicates: (1) the compatibilizer should be miscible with the polypropylene matrix, and (2) it should include a certain amount of polar functional groups in a molecule. Generally, the polypropylenes modified with maleic anhydride (MA) fulfill the two requirements and are frequently used as compatibilizer for polypropylene nanocomposites. However, they have mechanical properties lower than the native polypropylene, due to chain scission during grafting. Therefore, the addition of PP-g-MA can result in lower mechanical properties of the final composite. Hence, it is important to investigate the effect of PP-g-MA on the degree of dispersion, to optimize its concentration.

The object of this study is to examine the effect of PP-g-MA concentration in the system polypropylene/organoclay and to characterize the influence of processing conditions on clay dispersion. The polypropylene-organoclay composites were prepared by direct melt intercalation method, both in internal mixer and twin screw extruder. The state of dispersion was analyzed by X-ray diffraction, transmission electron microscopy as well as melt rheometry.

2. Materials and methods

2.1. Materials

The organoclay used in this study (Cloisite®20A) is obtained from Southern Clay Products (Gonzales, TX). It is a Na^+-montmorillonite, chemically modified with dimethyl dihydrogenated tallow quaternary ammonium chloride, where N^+ denotes quaternary ammonium chloride and HT denotes hydrogenated tallow (Fig. 1). HT is made of approximately 65% $C_{18}H_{37}$, 30% $C_{16}H_{33}$ and 5% $C_{14}H_{29}$.

All polymers used in this study are obtained from Atofina. The homopolymer polypropylene (PPH5060) has a melt flow index of 6 g/10 min and a melting temperature of 164 °C. The compatibilizer is a maleic anhydride functionalized polypropylene (PP-g-MA), containing 1 wt% of maleic anhydride (OREVAC© C100). The MFI and the melting temperature of PP-g-MA are 10 g/10 min and 161 °C, respectively. The zero-shear viscosity of PP is 5400 Pa s at 200 °C. On the range of frequencies studied, the viscosity of PP-g-MA is 5–10 times lower.

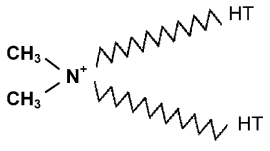

Fig. 1. Chemical structure of the dimethyl dihydrogenated tallow quaternary ammonium chloride.

2.2. Preparation of polypropylene-organoclay composites

The organoclay is dried at 100 °C for 12 h in a vacuums oven prior to compounding. Melt mixing of the samples is performed in an internal mixer (Haake Rheomix 600) equipped with roller rotors. A dry batch containing all three components is pre-mixed before introduction into the internal mixer, with a fill factor of 0.8. In a first set, we examine the effect of compatibilizer by varying the concentration of PP-g-MA (from 0 to 40 wt%) with following conditions: rotor speed $N=100$ rpm, mixing time $t=10$ min and mixer temperature $T_{mix}=180$ °C. For comparison, the corresponding polymer pairs (PP/PP-g-MA) without organoclay are also prepared by melt mixing under the same conditions ($N=100$ rpm, $t=10$ min, $T_{mix}=180$ °C, fill factor = 0.8). In a second set, several formulations are chosen to investigate the influence of processing conditions. The processing variables studied are the rotor speed N (10–150 rpm), the mixing time t (5–30 min) and the mixer temperature T_{mix} (180 and 200 °C). These conditions are chosen to minimize the degradation of PP and PP-g-MA during processing.

Melt mixing of PP/PP-g-MA/Cloisite®20A composites are also studied using a twin screw extruder. The machine used is an industrial self-wiping co-rotating twin screw extruder, Clextral BC45 (Clextral, Firminy, France) with following characteristics: centerline distance 45 mm, screw diameter 50 mm, barrel length 1.2 m, $L/D=24$. The screw profile is indicated in Table 1. It is composed of a left-handed element for the melting, followed by three mixing zones, with different configurations of kneading blocks. Polypropylene and PP-g-MA pellets and nanoclay are tumble mixed and introduced simultaneously in the hopper.

Barrel temperatures (180 °C) and screw speed (200 rpm) are kept constant. Only the influence of feed rate (between 4 and 30 kg/h) is studied here.

It should be noted that the clay concentration is fixed at 5 wt% in all cases. The notation used in the following for defining the blend compositions is PP/PP-g-MA/Cloisite®20A, expressed in mass fraction.

2.3. Structure and morphological characterization

The structure of layered silicates and the morphology of composites are analyzed by wide angle X-ray scattering (WAXS) and transmission electron microscopy (TEM). X-ray diffraction (XRD) data are collected on a Philips X'Pert PRO with Cu K_α radiation of wavelength 1.54 Å. The accelerating voltage is 40 kV. Diffraction spectra are

Table 1
Screw profile used in the experiments, from die to hopper

100	50	50	100	100	50	200	50	200	50	50	200	Length (mm)
25	KB 5/90	KB 12.5/30	25	33.3	KB 12.5/90	33.3	KB 10/−45	50	−25	25	50	Pitch (mm)

KB 5/90 means a block of kneading discs of thickness 5 mm and staggering angle 90°; a negative pitch or angle corresponds to a left-handed element.

obtained over a 2θ range of 2–10° and the interlayer spacing (d_{001}) is calculated using the Bragg equation: $\lambda = 2d \sin \theta$, where λ is the wavelength. The samples are prepared as discs of 50 mm diameter and 1.5 mm thickness, by compression molding at 180°. Each measurement is repeated four times, on two different surfaces.

TEM observations are performed on a Philips CM12 with an accelerating voltage of 120 kV. The TEM samples, around 90 nm thick, are prepared from the material as taken out from the internal mixer, by using a cryo-microtom equipped with a diamond knife at −80 °C.

2.4. Rheological measurements

Rheological measurements are performed in small amplitude oscillatory shear on a parallel plate rheometer (Rheometrics RMS 800), using discs of 25 mm diameter and 1 mm thickness. As for XRD, test specimens are prepared by compression molding at 180°. Storage G' and loss modulus G'' are measured over a frequency range of 0.1–100 rad/s at 220 °C in a nitrogen environment. The samples are equilibrated for 15 min in the rheometer after loading, prior to testing. A strain sweep test is performed for each sample to ensure that the strain used is within the linear viscoelastic range.

3. Results and discussion

3.1. Effects of PP-g-MA concentration

Fig. 2 shows the series of X-ray diffraction spectra of original Cloisite®20A and PP/PP-g-MA/Cloisite®20A composites, in which the concentration of PP-g-MA varies from 0 to 40 wt%. We recall that the Cloisite®20A concentration is constant and equal to 5% wt. The interlayer spacing of Cloisite®20A is 2.51 nm before compounding. For the uncompatibilized system (95/0/5), the XRD pattern exhibits no significant increase in interlayer spacing (2.56 nm after mixing). This indicates that the polypropylene does not intercalate into the interlayer, even if the montmorillonite is modified with dimethyldihydrogenated tallow ammonium ions.

In contrast, for compatibilized systems, X-ray diffraction peaks are shifted to lower angles, indicating the increase in interlayer spacing by the intercalation of polymer. The results of interlayer spacing are summarized in Table 2. The interlayer spacing increases progressively, from 2.83 nm for 5 wt% compatibilizer to 3.11 nm for 15 wt% compatibilizer. However, in the range of 15–25 wt% compatibilizer, no significant increase in interlayer spacing is observed.

Over 25 wt% compatibilizer, the interlayer spacing could not be determined due to the peak broaden. Nevertheless, it should be noted that there is a peak characteristic of interlayer spacing, even it is small. The decrease in intensity and the broadening of peaks indicate that the stacks of layered silicates become more disordered, while maintaining a periodic distance. In addition, the decrease in intensity could be the result of a partial exfoliation of layered silicates.

It is well know that the rheological properties of nanocomposites are sensitive to the surface characteristics and state of dispersion of the dispersed phase. Therefore, rheometry can be envisaged as a powerful tool for characterizing the state of dispersion [11–13].

Fig. 3 shows the storage modulus of PP/PP-g-MA blends and PP/PP-g-MA/Cloisite®20A composites as a function of strain amplitude at $\omega = 1$ rad/s. Similar trends are observed for the loss modulus (not shown here). The PP/PP-g-MA binary blends display linear viscoelastic behavior until a strain amplitude of about 30%, practically independent of the amount of PP-g-MA. For the PP/PP-g-MA/ Cloisite®20A composites, however, the linear viscoelastic range decreases progressively when increasing PP-g-MA content. Since the concentration of organoclay in the nanocomposites is the same (5 wt%), the decrease in linear viscoelastic

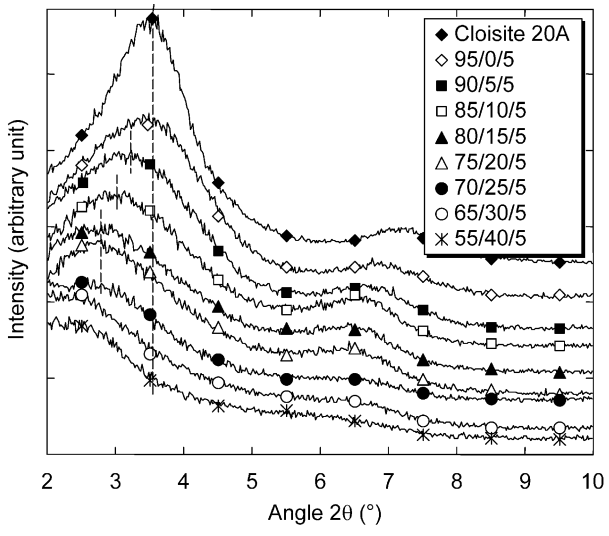

Fig. 2. XRD patterns of composites prepared with different amounts of PP-g-MA at $N = 100$ rpm, $T_{mix} = 180$ °C and $t = 10$ min.

Table 2
WAXS-Derived interlayer spacing for composite materials, calculated according to Fig. 2

Formulation (PP/PP-g-MA/Cloisite®20A)	*d*-spacing (nm)
Cloisite®20A	2.51
95/0/5	2.56
90/5/5	2.83
85/10/5	3.04
80/15/5	3.11
75/20/5	3.18
70/25/5	3.11
65/30/5	NA*
55/40/5	NA*

NA*: peak location is difficult to determine due to peak's broadness.

range of PP/PP-g-MA/Cloisite®20A can be attributed to the difference in the state of dispersion.

Fig. 4 shows the storage modulus G' and the complex viscosity $|\eta^*|$ as function of frequency for the PP/PP-g-MA blends. It is found that the low viscous PP-g-MA has mainly an effect of 'dilution' on polypropylene viscosity. No specific effect on the storage modulus at low frequency is observed, presumably indicating a good miscibility between

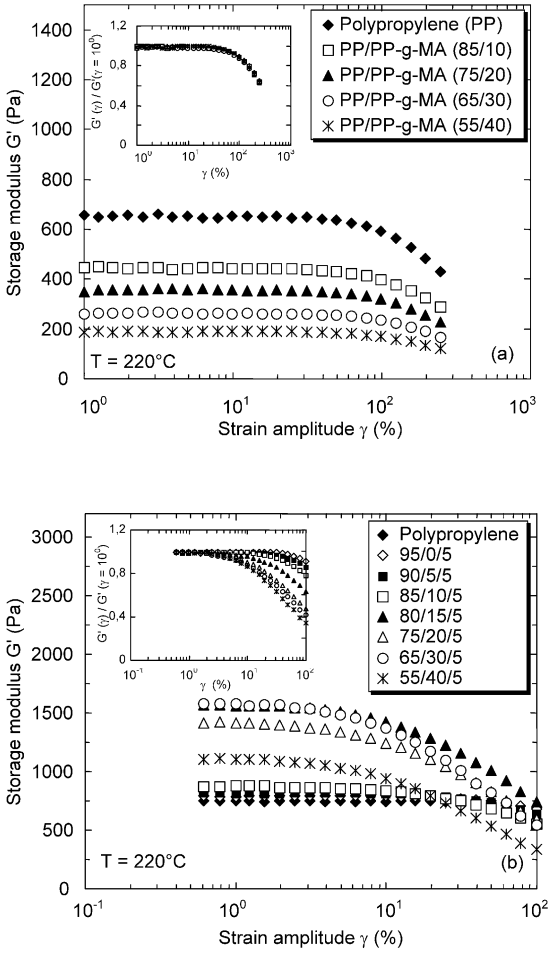

Fig. 3. Strain dependence of (a) PP/PP-g-MA blends and (b) PP/PP-g-MA/Cloisite®20A composites, measured at $T=220$ °C and $\omega=1$ rad/s.

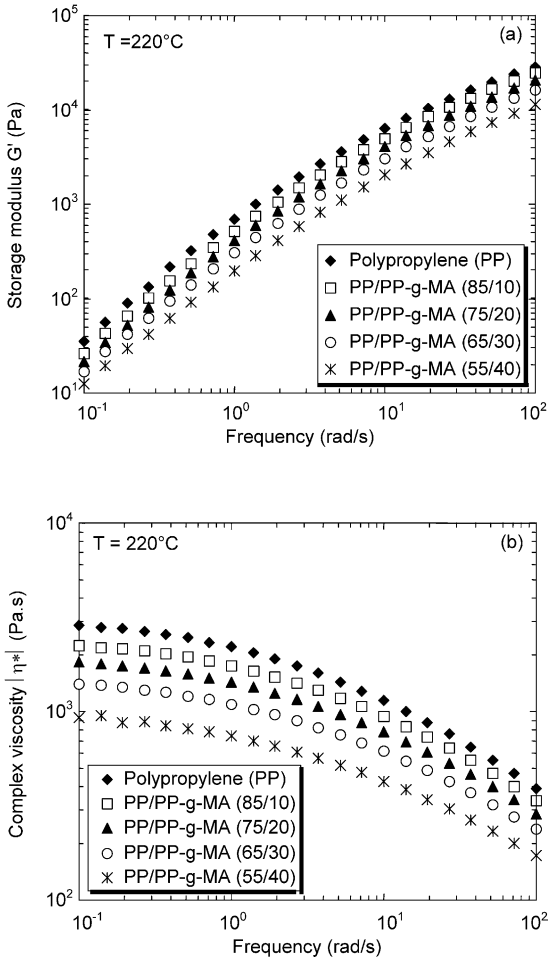

Fig. 4. (a) Storage modulus G' and (b) complex viscosity $|\eta^*|$ of PP/PP-g-MA blends prepared with different amounts of PP-g-MA at $N=100$ rpm, $T_{mix}=180$ °C and $t=10$ min.

PP and PP-g-MA. The rheological behavior of the binary blend that corresponds to the weight ratios present in the PP/PP-g-MA/Cloisite®20A composites will be used as reference matrix behavior.

Fig. 5 presents the storage modulus G' as function of frequency for the composites obtained with different concentrations of PP-g-MA. At frequencies higher than 10 rad/s, G' slightly decreases when the concentration of PP-g-MA increases. This is due to the fact that the viscosity of PP-g-MA is lower than that of polypropylene matrix as described above.

On the other hand, at low frequencies (lower than 1 rad/s), we observe an increase in the storage modulus G' when the concentration of PP-g-MA increases, with the onset of a plateau.

For 0 and 5 wt% PP-g-MA, the curves of G' do not show a significant change and are superimposed to the one of the pure polypropylene. In contrast, at concentration of PP-g-MA between 10 and 25 wt%, the storage modulus dramatically increases with the concentration of PP-g-MA. According to Galgali et al. [12] and Solomon et al. [13], the

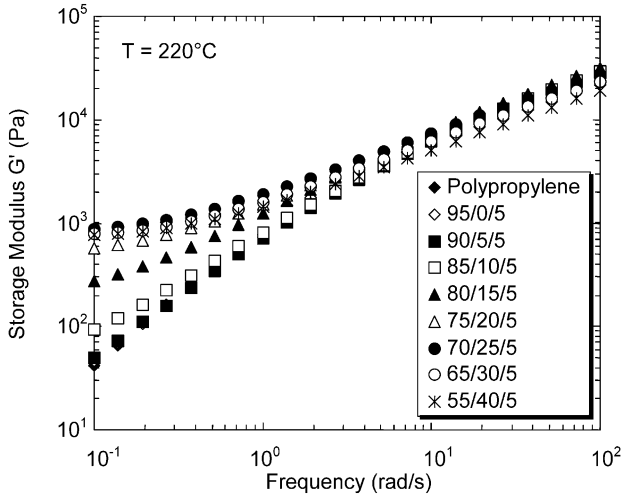

Fig. 5. Comparison of the storage modulus G' of PP/PP-g-MA/Cloisite®20A composites prepared with different amounts of PP-g-MA at N = 100 rpm, T_{mix} = 180 °C and t = 10 min.

increase in storage modulus at low frequency, which does not exist for the corresponding matrices, could be explained by the existence of a percolated network microstructure. Therefore, it is reasonable to say that the state of exfoliated silicate layers increases with the increase in compatibilizer amount in this concentration interval. Finally, over 25 wt% compatibilizer, the storage modulus does not significantly increase with PP-g-MA. Therefore, it could be considered that the state of exfoliation remains identical.

Fig. 6(a) shows the complex viscosity for different amounts of PP-g-MA. Like the storage modulus, the complex viscosity is identical to those of the pure polypropylene for PP-g-MA lower than 5 wt% and increases progressively at low frequency with the increase in PP-g-MA, for reaching a maximum at 25 wt%. Above 25 wt%, the complex viscosity slightly decreases, due to the low viscosity of PP-g-MA.

The increase in complex viscosity at low frequency can be compared to those of a material exhibiting a yield stress. For describing this behavior, we propose a Carreau–Yasuda model with yield stress, which was successfully used by Berzin et al. [14] to describe the changes in rheological properties during the peroxide degradation of polypropylene copolymers:

$$\eta s(\omega) = \frac{\sigma_0}{\omega} + \eta_0[1 + (\lambda\omega)^a]^{(m-1)/a} \quad (1)$$

where σ_0 is the yield stress, η_0 is the zero shear viscosity, λ is the time constant, a is the Yasuda parameter and m is the dimensionless power law index. These five parameters were adjusted for obtaining the best fit with the experimental data.

Fig. 6(b) shows the superposition between the experimental data and the fit curve of $|\eta^*|$ by Eq. (1). The agreement is excellent. The parameters obviously vary with PP-g-MA content. However, some parameters, such as time

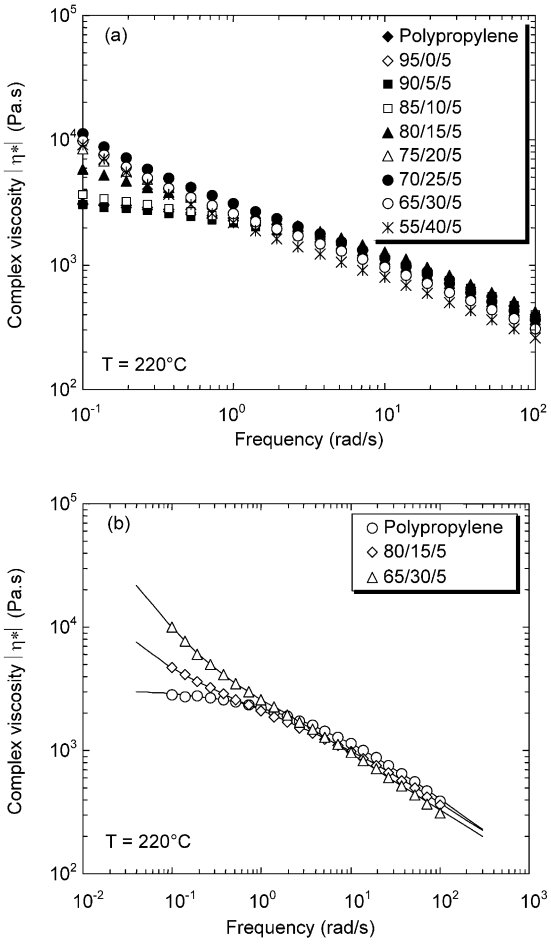

Fig. 6. (a) Comparison of the complex viscosity $|\eta^*|$ of PP/PP-g-MA/Cloisite®20A composites prepared with different amounts of PP-g-MA at N = 100 rpm, T_{mix} = 180 °C and t = 10 min and (b) empirical fitting of complex viscosity $|\eta^*|$ with Eq. (1).

constant λ or dimensionless power law index m, do not significantly change: m increases from 0.4 to 0.6 and λ from 0.3 to 0.9, when PP-g-MA increases from 0 to 40 wt%. The most interesting and important parameter is the yield stress σ_0. Fig. 7 shows the plot of the yield stress as function of PP-g-MA amount. The interlayer spacing from Table 2 is also plotted to compare the effect of PP-g-MA on the state of intercalation and exfoliation.

At low PP-g-MA content (<10 wt%), the interlayer spacing increases, while the yield stress is practically zero, suggesting that most of the layer silicates are intercalated by polymer, but quite no individual layer is separated from the tactoids. For PP-g-MA between 10 and 25 wt%, the interlayer spacing slightly increases until 15 wt% and then remains constant, while the yield stress dramatically increases. These results indicate that the corresponding morphologies are intercalated composites, with increasing individual layers separated from the stack layers. The proportion of exfoliation is more and more important when PP-g-MA increases. This is coherent with the decreasing in intensity observed in XRD patterns (Fig. 2). Above 25 wt%

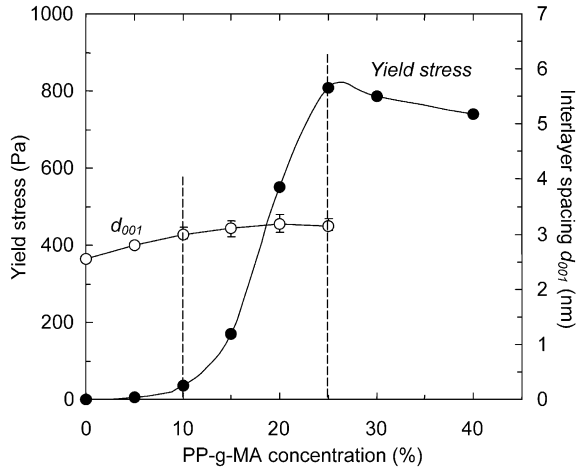

Fig. 7. Comparison of interlayer spacing and melt yield stress at 220 °C as a function of PP-g-MA loading for the PP/PP-g-MA/Cloisite®20A composites prepared at $N = 100$ rpm, $T_{mix} = 180$ °C and $t = 10$ min.

PP-g-MA, the yield stress is practically constant. Therefore, it is reasonable to conclude that, in these processing conditions, the maximum exfoliation has been reached.

In order to confirm the composite structures, the morphology was observed by TEM. Fig. 8 shows TEM micrographs (at magnification of 10,000) of the composites containing 0, 5, 15, and 30 wt% of PP-g-MA. Without PP-g-MA, we observe the clay aggregates at a micrometer level. Practically, no individual silicate layer is dispersed. For the hybrids containing PP-g-MA, we clearly observe that the size of aggregates is greatly reduced, although some aggregates still exist. The existence of the small peaks in the XRD patterns should be attributed to these aggregates. In best conditions (30 wt%), the individual silicate layers are really observed at high magnification (100,000), as shown in Fig. 9, corresponding to the partial exfoliation of the clay.

3.2. Effect of mixing time

Fig. 10 shows the effect of mixing time for the formulation 80/15/5, realized at a rotor speed of 50 rpm and at a temperature of 180 °C. XRD patterns show that the peak position remains quite constant (interlayer spacing varies between 3.11 and 3.32 nm), suggesting that the state of intercalation is completely obtained in 5 min of mixing.

An important difference, however, is observed in the storage modulus G' and complex viscosity $|\eta^*|$ as shown in

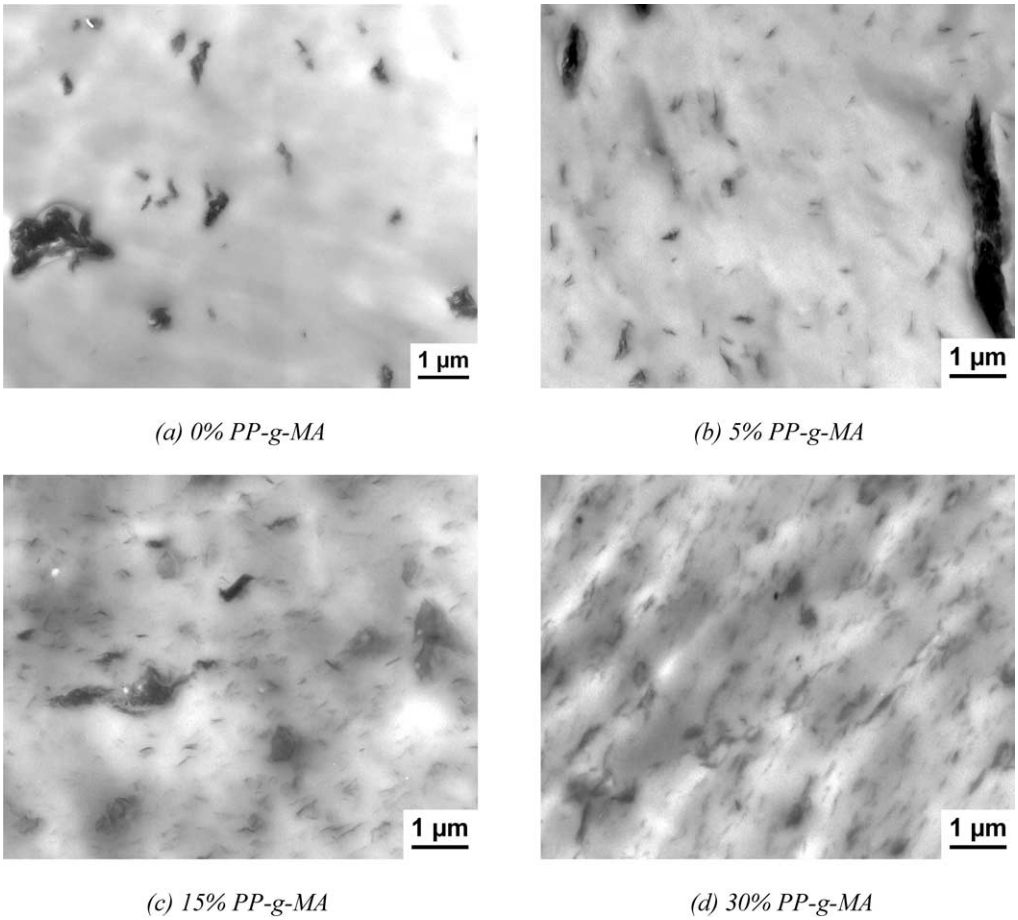

(a) 0% PP-g-MA (b) 5% PP-g-MA

(c) 15% PP-g-MA (d) 30% PP-g-MA

Fig. 8. TEM micrographs (×10,000) of PP/PP-g-MA/Cloisite®20A composites with different PP-g-MA content, prepared at $N = 100$ rpm, $T_{mix} = 180$ °C and $t = 10$ min.

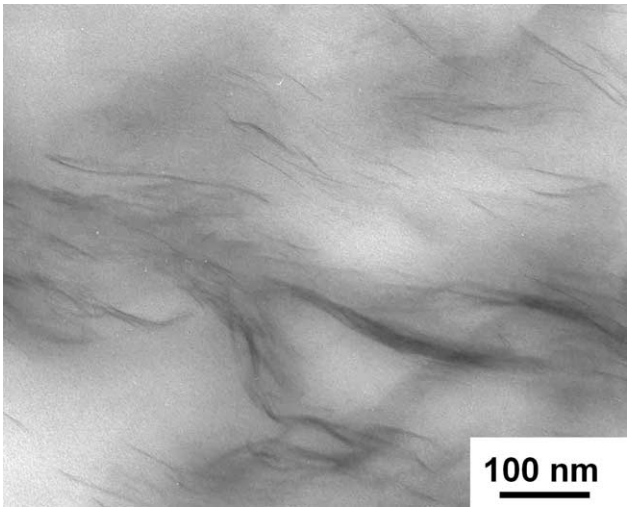

Fig. 9. TEM micrograph (×100,000) of the composite with 30 wt% PP-g-MA, prepared at $N=100$ rpm, $T_{mix}=180$ °C and $t=10$ min.

Fig. 11: the low frequency values, and thus the degree of dispersion, are improved when the mixing time increases, at least up to 20 min. It should be noted that the torque recorded during mixing reaches a steady state after 5 min. No further change with time is observed, indicating that no degradation occurs during sample preparation. The melt yield stress calculated by fitting the complex viscosity data with Eq. (1) (Fig. 11(b)) increases from 84 Pa at 5 min to 230 Pa at 10 min and finally 456 Pa and 420 Pa at 20 and 30 min, respectively. This suggests that the time needed to achieve a maximum quality of dispersion is much longer than the one to obtain a complete intercalation.

3.3. Effect of rotor speed

Fig. 12 presents XRD patterns for the formulation 80/15/5 with various rotor speeds, from 10 to 150 rpm. Mixing time and temperature are fixed at 10 min and 180 °C, respectively.

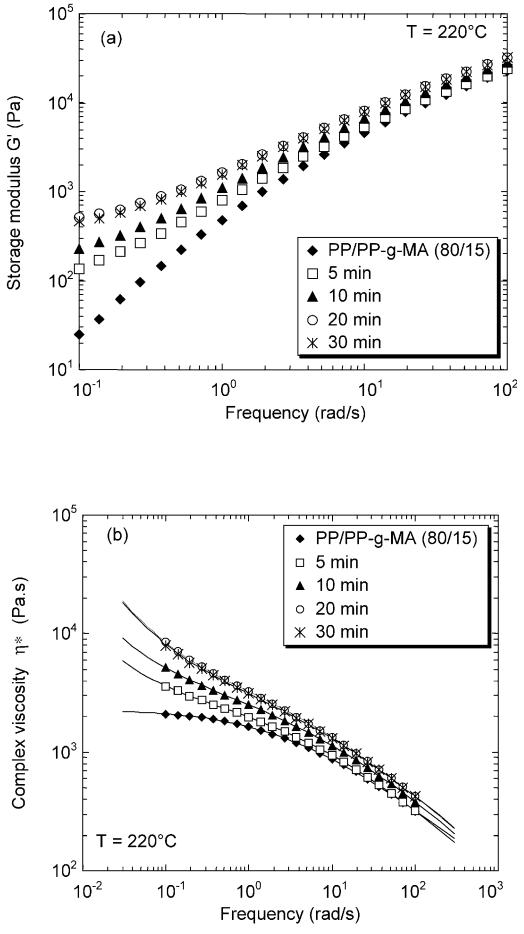

Fig. 11. (a) Storage modulus G' and (b) complex viscosity $|\eta^*|$ of PP/PP-g-MA/Cloisite®20A (80/15/5) composites prepared with various mixing times at $N=50$ rpm and $T_{mix}=180$ °C. The solid curves on the complex viscosity $|\eta^*|$ represent the empirical fitting with Eq. (1).

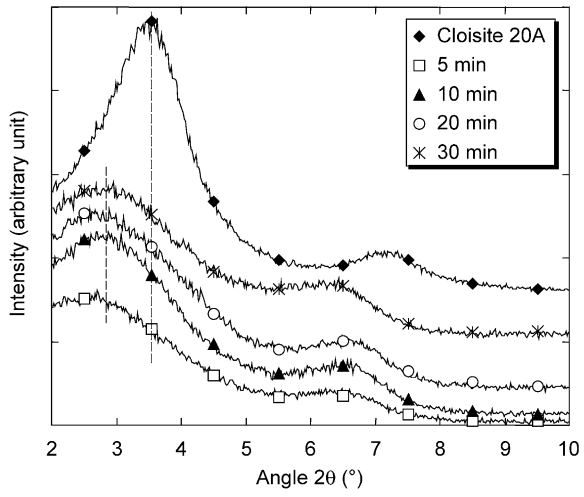

Fig. 10. XRD pattern of PP/PP-g-MA/Cloisite®20A (80/15/5) composites prepared with various mixing times at $N=50$ rpm and $T_{mix}=180$ °C.

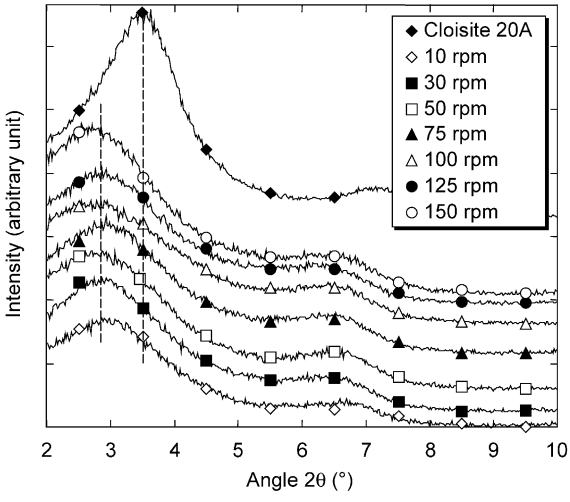

Fig. 12. XRD patterns of PP/PP-g-MA/Cloisite®20A (80/15/5) composites prepared with various rotor speeds at $T_{mix}=180$ °C and $t=10$ min.

We observe that the peak position does not significantly change with rotor speed. The interlayer spacing varies between 3.03 and 3.25 nm, indicating that the intercalation does not significantly depend on the shear rate. We observe similar results with the other PP-g-MA amounts (5–25 wt%).

In contrast, the rotor speed has a great influence on the state of exfoliation, as illustrated in Figs. 13 and 14 for the formulations 80/15/5 and 65/30/5, respectively. The degree of exfoliation is increased when increasing the rotor speed and significantly depends on the PP-g-MA content: the effect is enhanced at higher content.

This effect can be described through the value of the melt yield stress (Eq. (1)) as shown in Fig. 15 where the calculated melt yield stress at 220 °C is plotted as a function of rotor speed, for PP-g-MA amounts of 15 and 30 wt%. We found that the yield stress, corresponding to the state of exfoliation, increases with rotor speed, then stabilizes beyond a certain value (50 rpm for 15 wt% and 100 rpm for 30 wt% PP-g-MA). The increase in PP-g-MA is favorable to this mechanism: the optimal value of melt yield stress is multiplied by a factor four when PP-g-MA amount increases from 15 to 30 wt%.

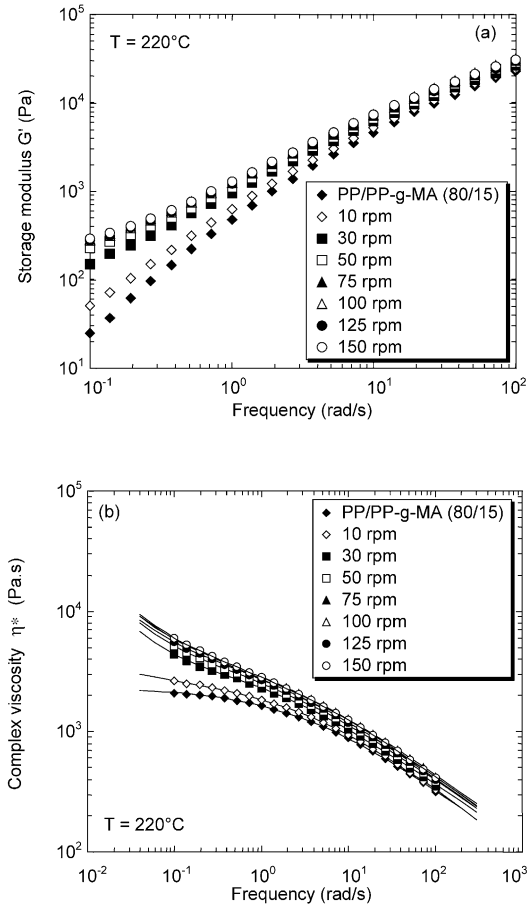

Fig. 13. (a) Storage modulus G' and (b) complex viscosity $|\eta^*|$ of PP/PP-g-MA/Cloisite®20A (80/15/5) composites prepared with various rotor speeds at $T_{mix}=180$ °C and $t=10$ min. The solid curves on the complex viscosity $|\eta^*|$ represent the empirical fitting with Eq. (1).

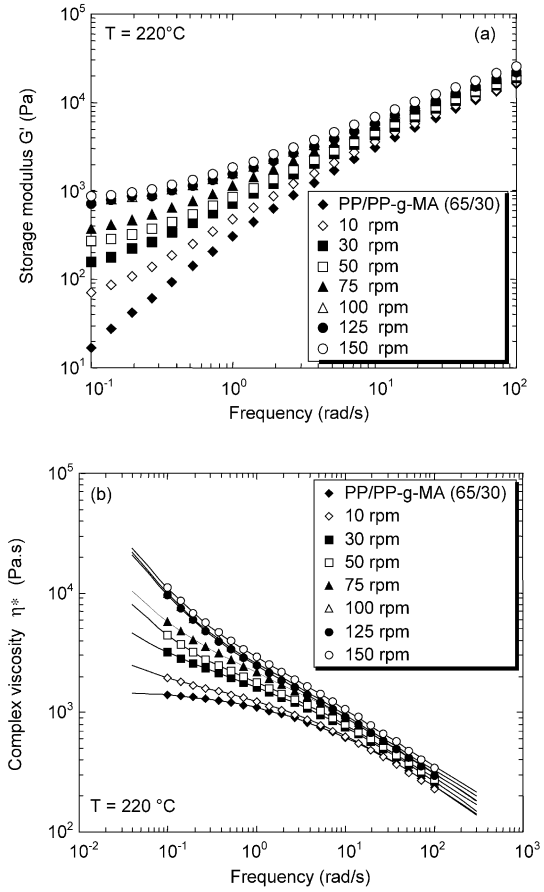

Fig. 14. (a) Storage modulus G' and (b) complex viscosity $|\eta^*|$ of PP/PP-g-MA/Cloisite®20A (65/30/5) composites prepared with various rotor speeds at $T_{mix}=180$ °C and $t=10$ min. The solid curves on the complex viscosity $|\eta^*|$ represent the empirical fitting with Eq. (1).

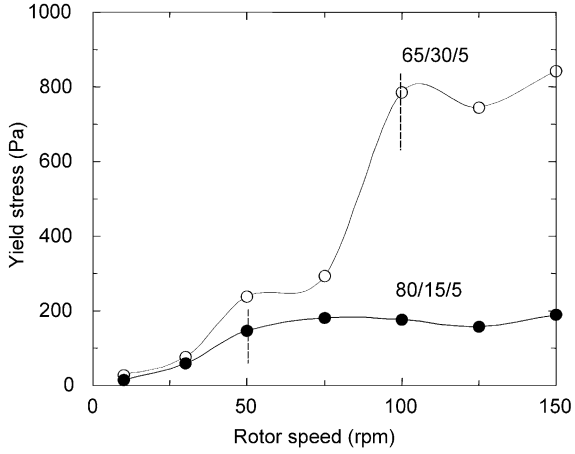

Fig. 15. Comparison of the evolution of melt yield stress at 220 °C as a function of rotor speed for two different formulations of PP/PP-g-MA/Cloisite®20A composites. The samples are prepared at $T_{mix}=180$ °C and $t=10$ min.

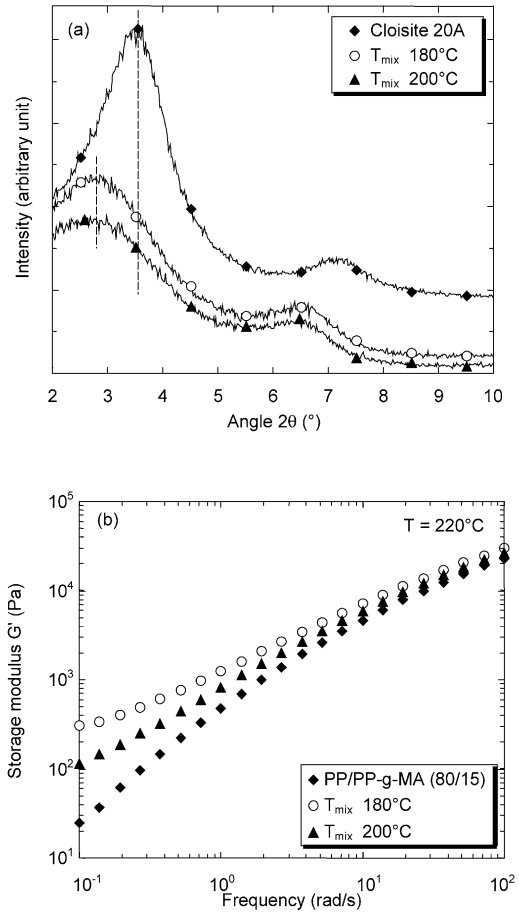

Fig. 16. (a) XRD pattern and (b) storage modulus G' for PP/PP-g-MA/Cloisite®20A (80/15/5) composites prepared at two mixing temperature, 180 and 200 °C, at rotor speed $N=50$ rpm and mixing time $t=10$ min.

3.4. Effect of mixing temperature

Fig. 16(a) presents XRD patterns for the formulation 80/15/5 at two mixing temperatures, 180 and 200 °C ($N=50$ rpm, $t=10$ min). They show that the peak position does not change with mixing temperature. This indicates that the degree of intercalation is independent of the temperature, in the range investigated. As the interlayer spacing is higher than for native Cloisite®20A, we may conclude that the quaternary ammonium ions are not degraded during the intercalation process: if the temperature is higher, chain diffusion is more rapid and allows intercalation before eventual degradation of the quaternary ammoniums. On the other hand, the operating temperature has a significant effect on the degree of exfoliation (Fig. 16(b)). The storage modulus G' measured at 220 °C is higher for composites prepared at 180 °C as compared to composites prepared at 200 °C. This indicates that a low mixing temperature leads to a higher degree of exfoliation. This can be explained by the level of stress applied during mixing, which is decreased when the temperature increases. The mixing temperature seems to have an influence on the shear stress, rather than on the diffusion of polymer chains.

4. Application to twin screw extrusion

We have until now studied the dispersion of layered silicates using an internal mixer, to elucidate the effects of various processing parameters. In this section, we will present the results of a preliminary study on the dispersion of layered silicates using an industrial self-wiping co-rotating twin screw extruder. The formulation used is 80/15/5.

Fig. 17 shows XRD patterns of composites extruded at different feed rates. Compared to the native clay, it is observed that the peak d_{001} is shifted towards lower angles. The interlayer spacing is increased from 2.51 nm (Cloisite®20A) to 3.1 nm. However, the value of interlayer spacing does not change with feed rate, suggesting that complete intercalation has occurred, although the mixing time in the twin screw extruder is very short at high feed rate (around 63 s at 30 kg/h). In addition, the value of interlayer spacing obtained by extrusion is comparable to that obtained from the internal mixer at the same formulation. We recall that no significant change on the interlayer spacing with the operating conditions was observed in the internal mixer. Therefore, it is quite reasonable to conclude that the state of intercalation is independent of the processing conditions.

On the other hand, the rheological measurements (Fig. 18(a) and (b)) show that the feed rate has a great influence on the exfoliation of layered silicates. The best dispersion is obtained at low feed rate. The melt yield stress calculated by fitting the complex viscosity data with Eq. (1) (Fig. 18(b)) increases from 239 Pa at 30 kg/h to 576 Pa at 14 kg/h and finally 2040 Pa at 4 kg/h. The effect of feed rate might be explained by the mean residence time, which is longer at low feed rate: it varies from 290 s at 4 kg/h to 63 s at 30 kg/h. We have already seen that the increase in mixing time improved the degree of exfoliation on the internal mixer. However, the mixing time is not the only one parameter

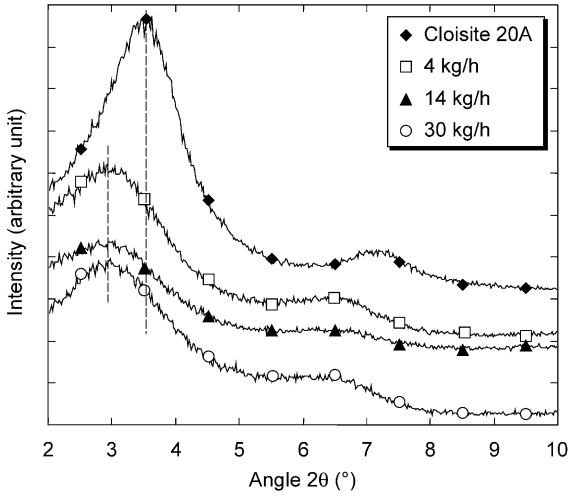

Fig. 17. Comparison of XRD patterns of PP/PP-g-MA/Cloisite®20A (80/15/5) composites prepared at various feed rates using the twin screw extruder at screw speed 200 rpm and barrel temperatures 180°C.

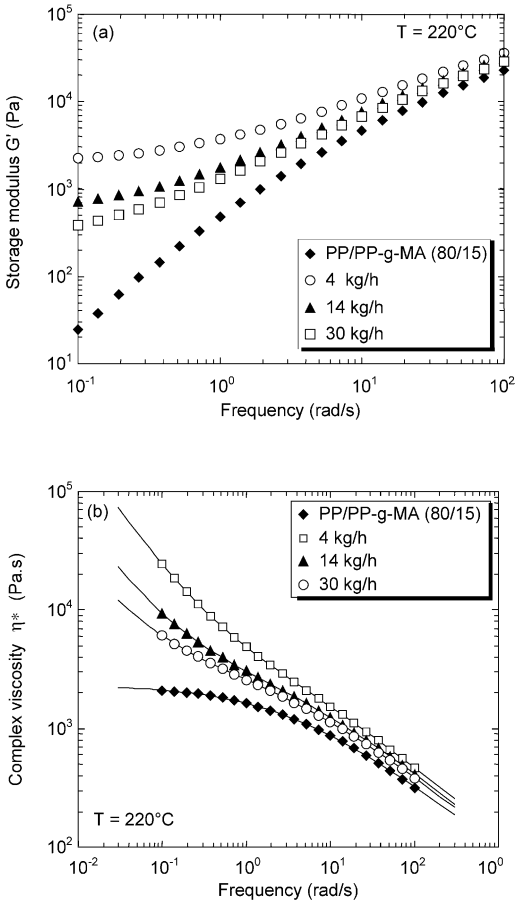

Fig. 18. (a) Storage modulus G' and (b) complex viscosity $|\eta^*|$ of PP/PP-g-MA/Cloisite®20A (80/15/5) composites prepared at various feed rates using the twin screw extruder at screw speed 200 rpm and barrel temperature 180 °C.

affecting the degree of dispersion. The shear intensity is also an important parameter as described in the Section 3.3. With the same formulation, we could obtain the better results using the twin screw extruder, indicating that the amount of PP-g-MA used can be minimized by optimizing the processing conditions as well as the screw profile.

5. Conclusion

Polypropylene nanocomposites have been prepared via direct melt intercalation by using an internal mixer and a co-rotating twin screw extruder. The degree of dispersion is improved by incorporating a maleic anhydride grafted polypropylene (PP-g-MA). However, this improvement is obtained for concentrations of PP-g-MA higher than 10 wt%. The clay aggregates become smaller and silicate layers are finely dispersed, as the ratio of PP-g-MA increases. However, no further improvement on the dispersibility is observed for PP-g-MA content above 25 wt%. The effects of processing parameters are also investigated. The state of intercalation, interpreted by interlayer spacing, is globally unaffected by processing parameters. Increasing shear stress, mixing time and decreasing mixing temperature improve clay layer silicate exfoliation. The proportion of exfoliation is characterized by rheological measurements. A Carreau–Yasuda model with yield stress is used to describe the behavior at low frequency. It is shown that the yield stress value is directly correlated to the degree of exfoliation of nanocomposites.

Acknowledgements

Polymers used in this study (polypropylene, PP-g-MA) were kindly provided by ATOFINA, which is gratefully acknowledged. We also thank M.Y. Perrin (CEMEF) for his precious help in Transmission Electron Microscopy.

References

[1] Alexandre M, Dubois P. Mater Sci Eng 2000;28:1–63.
[2] Ray SS, Okamoto M. Prog Polym Sci 2003;28:1539–641.
[3] Giannelis EP, Krishnamoorti R, Manias E. Adv Polym Sci 1998;138:107–47.
[4] Marchant D, Krishnamurthy J. Ind Eng Chem Res 2002;41:6402–8.
[5] Moore DM, Reynolds RC. X-Ray diffraction and the identification and analysis of clay minerals. Oxford: Oxford University Press; 1997.
[6] Fornes TD, Yoon PJ, Hunter DL, Keskkula H, Paul DR. Polymer 2002;43:5915–93.
[7] Le Pluart L, Duchet J, Sauterau H, Gérard JF. J Adh 2002;78:645–62.
[8] Kawasumi M, Hasegawa N, Kato M, Usuki A, Okada A. Macromolecules 1997;30:6333–8.
[9] Kato M, Usuki A, Okada A. J Appl Polym Sci 1997;66:1781–5.
[10] Hasegawa N, Kawasumi M, Kato M, Usuki A, Okada A. J Appl Polym Sci 1998;67:87–92.
[11] Ren J, Silva AS, Krishnamoorti R. Macromolecules 2000;33:3739–46.
[12] Galgali G, Ramesh C, Lele A. Macromolecules 2001;34:852–8.
[13] Solomon MJ, Almusallam AS, Seefeldt KF, Somwangthanaroj A, Varadan P. Macromolecules 2001;34:1864–72.
[14] Berzin F, Vergnes B, Delamare L. J Appl Polym Sci 2001;80:1243–52.